GaitWay: Monitoring and Recognizing Gait Speed Through the Walls

Chenshu Wu, *Member, IEEE*, Feng Zhang, *Member, IEEE*, Yuqian Hu, *Student Member, IEEE*, and K. J. Ray Liu, *Fellow, IEEE*

Abstract—Interests in monitoring and recognizing gait have surged significantly over the past decades. Traditional approaches rely on camera array, floor sensors (e.g., pressure mats), or wearables (e.g., accelerometers), none of which are suitable for continuous and ubiquitous everyday use. In this article, we present GaitWay, the first system that monitors and recognizes an individual's gait through the walls via wireless radios. GaitWay passively and unobtrusively monitors an individual's gait speed by a single pair of commodity WiFi transceivers, without requiring the user to wear any device or walk on a restricted walkway. On this basis, GaitWay automatically identifies stable walking periods, extracts physically plausible and environmentally irrelevant speed features, and accordingly recognizes a subject's gait. Built upon a distinct rich-scattering multipath model, GaitWay can capture one's gait speed when one is >10 meters away behind the walls. We conduct experiments in a typical indoor space and perform eight sessions of data collection with 11 subjects across six months, resulting in $>5{,}000$ gait instances. The results show that GaitWay achieves a median 0.12 m/s and 90%tile 0.35 m/s error in speed estimation, with a mean error of 3.36 cm in stride lengths. Further, it achieves a verification rate of 90.4% and a recognition rate of 81.2% for five users and 69.8% for 11 users, confirming its comfort and accuracy for continuous and ubiquitous use.

Index Terms—Gait recognition, WiFi sensing, speed estimation, human identification

1 Introduction

Gait, an individual's way of walking, is increasingly perceived as not only an essential vital sign [14], [30] but also an effective biometric marker [8]. On the one hand, gait, in particular, the walking speed, is considered as a valid and sensitive measure appropriate for monitoring and assessing functional decline and general health [14], [30], leading to its designation as *the sixth vital sign*. Gait reflects both functional and physiological changes, and is indicative and predictive of many health statuses, including mobility disability, response to rehabilitation, falls, and cognitive decline, etc [30]. Progression of gait is related to clinically meaningful changes in life quality and health conditions. Therefore, continuous monitoring of gait at home, rather than occasionally in-hospital clinical testing, is of great interest to an individual's healthcare.

On the other hand, gait provides distinctive biometric features of an individual, underlying a promising way of human identification. As a complex functional activity, many factors influence one's gait, rendering it as a unique behavioral trait. Research has shown that gait recognition could be even more reliable than face recognition [41], because there are tens of identifying characteristics entangled in gait, making it extremely difficult, if possible, to impersonate someone else's walking patterns. Compared with other human recognition systems, gait recognition is particularly attractive since it can operate remotely, passively, and non-intrusively, without any active cooperation of individuals.

Existing gait measurement and recognition systems usually rely on cameras [18], floor sensors [41], and/or wearables [8] to capture gait information. The target subjects have to either walk within restricted areas (typically only an instrumented walkway) or wear body sensors (e.g., accelerometers). Therefore, they are mainly limited to research and clinical usage and are not convenient and comfortable enough for ubiquitous applications in smart homes and smart buildings.

In contrast to the above systems, we attempt to sense gait using ambient radio signals. Recently, a new type of gait recognition using wireless signals (e.g., WiFi) is on the horizon [49], [63], [67]. Existing approaches, however, either use specialized devices [20] or require subjects to walk on a predefined path in a predefined direction [49], [58], [62]. Hence they are only suitable for confined areas (e.g., a 5 m corridor-like narrow path [49]) with a strong Line-Of-Sight (LOS) condition. Moreover, most of the existing works do not measure physiological gait [27], [29], [58], [62], [63], [67]. They merely extract RF-based features that are related to walking motions, making them location- and environment-dependent since the RF features are entangled with the surrounding environments. And most importantly, none of these WiFi-based systems can work for Non-LOS (NLOS) scenarios.

In this paper, we present GaitWay, the first system that can monitor and recognize an individual's gait through the walls. Leveraging the pervasive WiFi signals, GaitWay works in a non-intrusive and contactless manner. There is no need to instrument the user's body or physical environments. The user is neither required to keep walking on a designated path.

• *The authors are with the University of Maryland, College Park, MD 20742 USA, and also with the Origin Wireless Inc. E-mail: {cswu, fzhang15, yhu1109, kjrliu}@umd.edu.*

Manuscript received 2 July 2019; revised 2 Jan. 2020; accepted 10 Feb. 2020. Date of publication 19 Feb. 2020; date of current version 5 May 2021. (Corresponding author: Chenshu Wu.) Digital Object Identifier no. 10.1109/TMC.2020.2975158

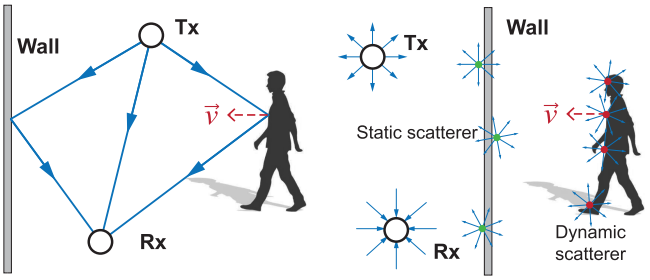

(a) Reflection model (b) Scattering model

Fig. 1. Multipath models for rich-scattering indoor environments. (a) Objects (e.g., a human body) are simplified as a single reflector producing only one major reflection path. (b) Objects scatter the signal and produce many paths.

In contrast, one can freely walk, turn, sit, or stand in the space. GaitWay will automatically estimate walking speeds, identify effective walking periods, and then extract gait characteristics for recognition, even when the user is as far as 10 meters away from the link or behind the walls. To achieve this, we overcome two critical challenges: *through-the-wall speed estimation* and *physical plausible gait feature extraction*.

First, it is extremely challenging to estimate real-time walking speed from radio signals. Previous approaches resort to specialized hardware with large bandwidths and many phased antennas [20]. Other approaches using commodity WiFi typically attempt to extract speed from Doppler effects [25], [40], [49]. The problems with Doppler effects, however, are two-fold: (1) It only reflects partial speed projected on a specific direction rather than the entire speed [39]; and (2) It is suitable only for narrow LOS area (typically within 4 to 5 m) [39], [49]. More generally speaking, we realize that the fundamental limitation of past works lies in the assumption of only a single dominate reflection path from the human body (known as the two-ray *reflection* model [47] as shown in Fig. 1a), which is unrealistic in rich-scattering indoor environments.

In contrast, we propose a *scattering* model (Fig. 1b), which treats environmental objects as multiple scatters. We mathematically reveal that, by the physics of electromagnetic field [19], the Channel State Information (CSI) statistically embodies the target's moving speed when accounting for a number of scattering multipaths. Built upon [60], we develop a statistical approach to derive speed from the autocorrelation function (ACF) of CSI, which leverages the statistical property of *all multipaths everywhere*, rather than a dominant one, and thus is independent of locations, heading directions, and the environments. Different from [60], we largely boost the sensing performance and coverage by *optimally* combining subcarriers using *Maximal Ratio Combining* (MRC) [43], thus allowing speed monitoring at a distance of up to 10 meters through the walls, which was only achieved by specialized devices previously. Furthermore, our model exploits extra phase information of CSI and is directly derived based on complex CSI.

Second, it is non-trivial to build an accurate and robust gait recognition system based on walking speed only. Conventional gait recognition systems usually extract salient characteristics dictated by body shape (e.g, silhouette by multi-view gait images) [18], [23], foot shape (e.g., underfoot pressure image by pressure mats) [7], [41], or multi-dimensional accelerations measured at diverse body locations [64], [66], all providing much richer information beyond walking speed. In GaitWay, however, only the walking speed is available, and the speed is captured without exerting any constraints to the subject's behaviors, making the recognition even challenging. We address this challenge by extracting various physically plausible and environmentally irrelevant features that characterize different perspectives of gait speed patterns, including gait symmetry, smoothness, variability, periodicity, etc., from the walking speed.

Putting it all together, we implement GaitWay on commodity off-the-shelf (COTS) WiFi devices and conduct experiments in a typical office space covering 5,000 ft^2. We collect eight sessions of data from 11 subjects on different days across six months. Most of the data are collected under NLOS conditions. GaitWay achieves a median 0.12 m/s and 90%tile 0.35 m/s error in gait speed monitoring, with a mean error of 3.36 cm for stride lengths, significantly outperforming previous WiFi-based approaches. GaitWay achieves a single user verification accuracy of 90.4% and a recognition rate of 93.7% for two users, which becomes 81.2% for five users and 69.8% for 11 users. The inspiring coverage and accuracy envision GaitWay as a new way for convenient gait monitoring and recognition in ubiquitous contexts.

In summary, we make the following contributions.

- We derive a statistical approach on top of a scattering multipath model for passive speed estimation, which can capture accurate speed when a target is over 10 meters away, or behind the walls.
- We build a gait speed monitoring and recognition system. By extracting a range of plausible physical features, GaitWay can recognize a subject independently from location, orientation, environments, and the user's apparel.
- We implement a prototype of GaitWay on COTS WiFi devices and conduct experiments in typical indoor spaces. The results confirm its accuracy and comfort for continuous and ubiquitous use.

The rest of the paper is organized as follows. We present the preliminaries on gait in Section 2. Speed estimation is introduced in Section 3, followed by gait extraction and recognition in Section 4. We present evaluation in Section 5, review the literature in Section 6 and conclude in Section 7.

2 Preliminaries on Gait Speed

Gait refers to the way of walking. Walking is a simple yet finely choreographed function, harmonizing many muscles over a complex bone and joint structure to deliver biomechanical locomotion. A gait cycle consists of two phases: the stance and swing phases, and further seven stages [23]. Gait, especially gait speed, can serve as a vital sign as well as a biometric cue.

Monitoring Gait as a Vital Sign. Gait has been shown to reflect health and functional status [14], [30]. Gait speed, also often termed walking speed, is the most important information being measured and concerned for healthcare. It has been recommended as a pragmatic and essential clinical

indicator of well-being [14]. Research findings have confirmed that gait speed is indicative and predictive of a range of outcomes, such as frailty [4], mobility disability [5], cognitive decline [1], falls [31], hospitalization [5], [31], as well as all-cause mortality [45]. Degradation in gait speed correlates with lower quality of life, increased risk in falls, and presence of depressive symptoms, etc. Due to its extensive predictive capabilities, gait speed was termed the sixth vital sign in 2009 [14], and after that, clinical and research practice continues to support this designation [30].

Gait monitoring is particularly crucial for eldercare since an increasing population of seniors is living alone (13 million in the US [35] and 6 million in Japan [36]) in today's aging society. For them, gait speed offers a passively measurable metric that is clinically interpretable for an assessment of fall risk, functional status, and ability to live independently, etc. A continuous and comfortable system for ubiquitous gait speed measurement, however, lacks.

Recognizing Gait as a Biometric Cue. Gait recognition has been studied since the late 1960s [9], [33]. Since then, a number of studies have objectively affirmed that gait is sufficiently consistent for a healthy individual and distinctive between individuals [8]. Gait recognition is particularly appealing for a range of ubiquitous applications that need human identification since it can be achieved at a distance without any active user cooperation. For example, a smart home would personalize the temperature and ambient light for a recognized user. A smart TV therein would react with her favorite programs. Smart home devices like Google Home and Amazon Alexa could directly interact with her in a more friendly way. For all of these to function, the user needs to do nothing but walk habitually inside the space. An easy-to-deploy and convenient system, however, is demanded for continuous and passive gait recognition.

Most existing gait recognition systems use extensive gait information, especially biomechanical features pertaining to the body's physical dimensions, shapes, and muscle contraction forces. For example, silhouettes from a video sequence [12], [17] and underfoot pressure images [14], [41] have been widely used. These systems are reliable, however, not economic and user-friendly.

In this work, we aim to build a system that continuously monitors and recognizes an individual's gait, without the need of exerting any constraints on the user, requiring any active cooperation from her, or instrumenting the walkway. The primary design goal of GaitWay is to provide everyday monitoring of gait speed as health data and enable recognition with gait speed alone for non-critical applications by reusing existing WiFi infrastructure. As a contactless and sensorless system, it would be attractive to various applications such as monitoring walking speed progression of elders living alone, recognition of family members in a house (e.g., for identifying a child from adults for TV content filtering), and automating personalized adjustment of environment conditions for an identified user, etc.

3 Speed Estimation Through the Walls

3.1 Rich Scattering Multipath Model

Limitation of Existing Models. Existing works on WiFi-based speed estimation rely on precise channel parameters, in particular, the Doppler Frequency Shift (DFS) [25], [40], [49], [50]. The limitations are two-fold.

First, as dictated by [39], DFS induced by human motion is not only related to the motion speed but also depends on the relative location and direction with respect to the link. Specifically, DFS only embodies the radial speed component projected on the normal direction of the ellipse with the Tx and Rx as foci. In an extreme case, if a user is walking on an ellipse with two foci at the locations of the Tx and Rx, no DFS will be observed, regardless of the walking speed.

Second, since DFS is a channel parameter of the reflection path, which is usually of magnitude weaker than a LOS path, it can be easily buried in channel noises and thus not perceivable, especially when numerous multipaths present. Because of this, all existing works are limited to only narrow areas in which both the Tx and Rx can see the moving target [25], [39], [40], [50].

More fundamentally speaking, existing approaches are based on a *reflection* model, as shown in Fig. 1a. The human body is simplified as a *single reflector*, producing only one dominant reflection path. DFS caused by human movements is then equivalently derived as the change rates of this particular reflection path [39], [50]. Such a two-ray reflection model, however, was developed for outdoor propagation and is unrealistic for rich multipath indoor environments [47]. Typically there are multiple reflection paths off a human body, which are, however, ignored. And the more multipaths there are, the worse such reflection models can work.

Proposed Rich Scattering Model. In contrast to past works, we investigate a distinct rich scattering model. As shown in Fig. 1b, the human body is seen as multiple *scatterers*, which reflect signals in diverse directions and superimpose at the Tx together with signals scattered by other objects via many paths. Given numerous multipaths, we do not geometrically analyze a specific reflection path nor assume a dominant one and ignore others. Instead, we statistically investigate the channel properties by accounting for *all multipaths* together. Our key finding is that, by the physics of EM fields, the target's moving speed can be calculated from the ACF of CSI. Built upon the statistical property of numerous multipaths, our method is independent of the environments, locations, and user orientations. In contrast to the previous reflection model that fails in rich multipath environments, the proposed model works even better with more multipaths and supports through-the-wall sensing.

3.2 Passive Speed Tracking

CSI Primer. Consider a wireless transmission pair, each equipped with omni-directional antennas. The channel frequency response (CFR), also called the channel state information, for the multipath channel at time t is generally modeled as

$$H(t,f) = \sum_{l=1}^{L} a_l(t) exp(-j2\pi f \tau_l(t)), \tag{1}$$

where $a_l(t)$ and $\tau_l(t)$ denote the complex amplitude and propagation delay of the lth multipath component (MPC), respectively, and L stands for the number of MPCs.

Due to the timing and frequency synchronization offsets and additive thermal noise, the real measurement of CFR $\tilde{H}(t,f)$ is expressed as

$$\tilde{H}(t,f) = \exp(-j(\alpha(t) + \beta(t)f))H(t,f) + n(t,f), \tag{2}$$

where $\alpha(t)$ and $\beta(t)$ are the random initial and linear phase distortions at time t, respectively.

Modeling Dynamic Scattering. In the following, we build a statistical model inspired by the physical properties of EM fields [19] and a previous work [60], which eventually allows us to derive speed from CSI. We present the core techniques but omit the detailed derivations due to space limitations.

The radio signals are scattered by numerous scatterers, such as walls, ceilings, floors, furniture, human bodies, etc. Due to the superposition principle of EM waves, the CSI $H(t,f)$ can be decomposed as

$$H(t,f) = \sum_{i\in\Omega_s(t)} H_i(t,f) + \sum_{j\in\Omega_d(t)} H_j(t,f) + \varepsilon(t,f), \tag{3}$$

where $\Omega_s(t)$ denotes the set of static scatterers, $\Omega_d(t)$ denotes the set of dynamic scatterers, and $H_i(t,f)$ stands for the part contributed by the ith scatterer. $\varepsilon(t,f)$ is the noise term, which can be approximated as additive white Gaussian noise (AWGN) with variance $\sigma^2(f)$ and is statistically independent of $H_i(t,f)$ [60]. The intuition behind the decomposition is that each scatterer can be treated as a "virtual Tx" diffusing the received EM waves in all directions, and then these EM waves add up together at the receive antenna after bouncing off the interior objects indoors. As a result, $H(t,f)$ actually measures the sum of the electric fields of all the incoming EM waves. In practice, within a sufficiently short period, it is reasonable to assume that both the sets $\Omega_s(t)$ and $\Omega_d(t)$ change slowly in time, and they can be approximated as time-invariant sets. Although past works based on the reflection model also divide multipaths into static and dynamic paths (rather than scatter sets) [39], [50], they assume only one dominate dynamic path, and the above statistical properties do not hold.

We consider a 2-D scattering model, where all the scatterers are within the same horizontal plane. Due to the channel reciprocity, EM waves traveling in both directions undergo the same physical perturbations (i.e., reflection, refraction, diffraction, etc.). Therefore, if the receiver were transmitting EM waves, the CSI "measured" at the ith scatterer or "virtual Tx" would be identical to $H_i(t,f)$. If the speed of the ith scatterer is v_i, then a continuous limit representation of $H_i(t,f)$ can be expressed as [19]

$$H_i(t,f) = \int_0^{2\pi} F_i(\theta,f)\exp(-jkv_i\cos(\theta)t)d\theta, \tag{4}$$

where $F_i(\theta,f)$ denotes the complex channel gain of the MPC from direction θ for the ith scatterer, and $k = \frac{2\pi}{\lambda}$ is the wave number where λ is the wavelength.

Statistical Derivation of Speed. Based on the well-established statistical theory of EM fields developed for reverberation cavities, which approximates indoor environments well, $F_i(\theta,f)$, for $\forall i$, can be represented as a random variable with the following properties [19]:

1) For $\forall\theta$, $F_i(\theta,f)$ is a circularly-symmetric Gaussian random variable with the same variance $\sigma_F^2(f)$;
2) For $\forall\theta_1 \neq \theta_2$, $F_i(\theta_1,f)$ and $F_i(\theta_2,f)$ are statistically independent;
3) For $\forall i \neq j \in \Omega_d$, $F_i(\theta_1,f)$ and $F_j(\theta_2,f)$ are statistically independent for $\forall\theta_1$ and $\forall\theta_2$.

With the above properties, now we investigate how the ACF of CSI relates to the speed v_i. The mean of $H_i(t,f)$ equals to zero, i.e., $\mathbb{E}[H_i(t,f)] = 0$, where $\mathbb{E}[\cdot]$ denotes the expectation operator. Then, the covariance of two CSIs with time lag τ can be written as [60]

$$\begin{aligned}\mathrm{Cov}[H_i(t,f), H_i(t+\tau,f)] &= \mathbb{E}\left[H_i(t,f)H_i^*(t+\tau,f)\right] \\ &= 2\pi\sigma_{F_i}^2(f)J_0(kv_i\tau),\end{aligned} \tag{5}$$

where $J_0(\cdot)$ is the 0th-order Bessel function of the first kind: $J_0(x) = \frac{1}{2\pi}\int_0^{2\pi}\exp(-jx\cos(\theta))d\theta$. The ACF of $H_i(t,f)$ with time lag τ, denoted as $\rho_{H_i}(\tau,f)$, is derived as

$$\begin{aligned}\rho_{H_i}(\tau,f) &= \frac{\mathrm{Cov}[H_i(t,f), H_i(t+\tau,f)]}{\mathrm{Cov}[H_i(t,f), H_i(t,f)]} \\ &= J_0(kv_i\tau).\end{aligned} \tag{6}$$

Similarly, the ACF of the CSI $H(t,f)$ with time lag τ, denoted as $\rho_H(\tau,f)$, can be obtained as

$$\begin{aligned}\rho_H(\tau,f) &= \frac{\mathrm{Cov}[H(t,f), H(t+\tau,f)]}{\mathrm{Cov}[H(t,f), H(t,f)]} \\ &= \frac{\sum_{i\in\Omega_d}\sigma_{F_i}^2(f)J_0(kv_i\tau) + \sigma^2(f)\delta(\tau)}{\sum_{i\in\Omega_d}\sigma_{F_i}^2(f) + \sigma^2(f)},\end{aligned} \tag{7}$$

where $\delta(\cdot)$ is the Dirac's delta function, which equals zero everywhere except for zero. As seen, $\rho_H(\tau,f)$ is a linear combination of the ACF of $H_i(t,f)$, and the weight of each term equals the energy scattered by that corresponding scatterer.

Consider that only one person is moving in the monitored area. The speeds of all the scatterers caused by the person are approximated to be the same, i.e., $v_i = v$, for $\forall i \in \Omega_d$. The rationale behind the approximation lies that the torso contributes most of the strong scatterers, which have similar speeds and dominate those from limbs with more different speeds. Thus by this assumption, the estimated speed is mainly the speed of the main body. Then, $\rho_H(\tau,f)$ can be simplified as

$$\begin{aligned}\rho_H(\tau,f) &= \frac{\sum_{i\in\Omega_d}\sigma_{F_i}^2(f) + \sigma^2(f)\delta(\tau)}{\sum_{i\in\Omega_d}\sigma_{F_i}^2(f) + \sigma^2(f)}J_0(kv\tau) \\ &\triangleq \alpha(f)J_0(kv\tau),\end{aligned} \tag{8}$$

where $\alpha(f)$ is defined as the gain of each subcarrier f. Equation (8) bridges the moving speed of the human body and the second-order statistics, i.e., ACF, of CSI.

In practice, the sample ACF is used instead, which is an estimate of the ACF, and we use $n(\tau,f)$ to stand for the estimation noise of the ACF, i.e.,

$$\hat{\rho}_H(\tau,f) = \alpha(f)J_0(kv\tau) + n(\tau,f). \tag{9}$$

Since the term $J_0(kv\tau)$ in (9) is a function of moving speed v, it's termed the *speed signal* in the following.

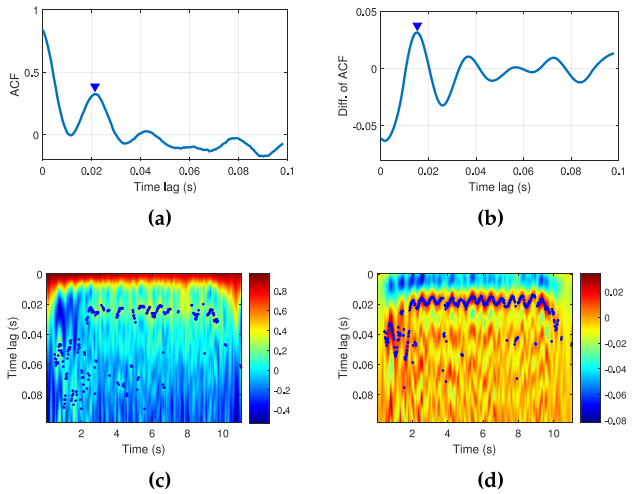

Fig. 2. Example of the combined speed signal. (a) Combined speed signal and (b) its difference; (c) Matrix of combined speed signals and (d) matrix of their differences.

Maximizing Speed Signal. From (9), one can derive the moving speed v from the ACF measurement $\hat{\rho}_H(\tau, f)$. In practice, however, the signal-to-noise ratio (SNR) of the speed signal on each subcarrier modulated by human movement can be pretty low, especially when the person being monitored is far away from the link or behind walls. As a second-order statistic, ACF circumvents the phase issue and is synchronized over all subcarriers, allowing direct combination of ACF measured on different subcarriers. In the following, we propose a novel scheme based on Maximal Ratio Combining [43] that combines the speed signals measured on multiple subcarriers in an optimal way such that the SNR of the speed signal is maximized. MRC is a classical diversity combining method in telecommunications that optimizes SNR by combining signals received on multiple antennas [43]. MRC is applicable here by treating subcarriers as the receiving diversity, which has been utilized to facilitate breathing estimation from WiFi [61].

When $\alpha(f)$ is small, i.e., $H(t, f)$ is dominated by the white noise, each tap of the ACF follows a zero-mean normal distribution with equal variance $1/N$ [42], i.e., $n(\tau, f) \sim \mathcal{N}(0, 1/N)$, where N is the number of samples used in the ACF estimation. Therefore, the variance of $n(\tau, f)$ in (9) is the same for different subcarriers. Because the noise terms of different subcarriers are statistically independent, it can be shown that the MRC scheme achieves the maximum of the SNR of the speed signal $J_0(kv\tau)$ [43], i.e.,

$$\begin{aligned} S(\tau) &= \sum_{f \in \mathcal{F}} w^*(f) \hat{\rho}_H(\tau, f) \\ &= \left(\sum_{f \in \mathcal{F}} w^*(f) \alpha(f) \right) J_0(kv\tau) + \sum_{f \in \mathcal{F}} w^*(f) n(\tau, f), \end{aligned} \tag{10}$$

where $S(\tau)$ is called the combined speed signal, $w^*(f)$ denotes the optimal combining weight for subcarrier f, and $w^*(f)$ is linearly proportional to the gain $\alpha(f)$.

The gain $\alpha(f)$ on each subcarrier, however, is not directly available from CSI. Fortunately, since $J_0(kv\tau)$ is continuous at time lag 0, i.e., $\lim_{\tau \to 0} J_0(kv\tau) = 1$, we have $\alpha(f) = \lim_{\tau \to 0} \rho_H(\tau, f)$ according to (8). Therefore, when the channel sampling rate F_s is sufficiently high, $\alpha(f)$ can be estimated as the quantity $\hat{\rho}_H(\tau = 1/F_s, f)$, the first tap of the ACF, and $w^*(f)$ is taken as

$$\hat{w}^*(f) = \hat{\rho}_H(\tau = 1/F_s, f), \tag{11}$$

where the sample ACF $\hat{\rho}_H(\tau, f)$ is directly calculated from the CSI measurements.

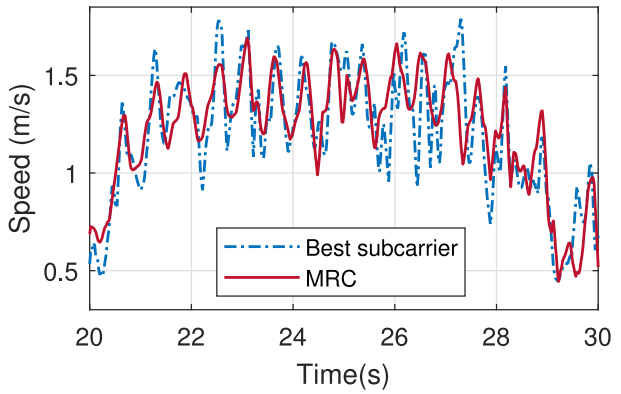

Fig. 3. Speed estimation with MRC.

The intuition that MRC maximizes the SNR is that, when combining all subcarriers appropriately, the "good" subcarriers will boost the signal while the "bad" subcarriers will help attenuate the noise since their noise terms are independent. The MRC is a key improvement over our previous work [60] and largely boosts the sensing coverage.

Calculating Speed. Fig. 2a shows an example of the combined speed signal, and Fig. 2c shows the matrix of the combined speed signal, where each column of the matrix corresponds to a combined speed signal. As we can see from the Fig. 2a, the shape of the combined speed signal resembles the Bessel function $J_0(x)$ with $x = kv\tau$, and the speed v can be thus extracted by matching their key characteristics, e.g., the locations of the first peak or valley. We use the first peak in GaitWay, i.e., the speed is calculated as

$$\hat{v} = \frac{x_0}{k\hat{\tau}} = \frac{x_0 \lambda}{2\pi\hat{\tau}}, \tag{12}$$

where x_0 is a constant value corresponding to the first peak of Bessel function $J_0(x)$, and $\hat{\tau}$ is the time lag corresponding to the first peak in the combined speed signal, as marked by the blue dots in Fig. 2c.

In practice, two steps are further taken to enhance speed estimation. First, to facilitate peak finding, the difference of the combined speed signal is used, as shown in Fig. 2b, which is more evident than Fig. 2d. In this case, x_0 becomes the location corresponding to the first peak of the derivative of $J_0(x)$. Second, we use the phase difference between two receive antennas to eliminate errors in the raw phase [40]. Note that, thanks to ACF, our approach is insensitive to the initial phase offsets [53]. Fig. 3 shows the speed estimates of a 10s period during a user's continuous walking. Fig. 3 also shows that MRC largely enhances the speed estimation.

Comparing With DFS. We implement the DFS-based method [39], [49] and compare it with the proposed approach by real measurements. To compare in both LOS and NLOS cases, we set up two links with one Tx and two Rx in a line, one with LOS condition (10 m away) and the other behind a

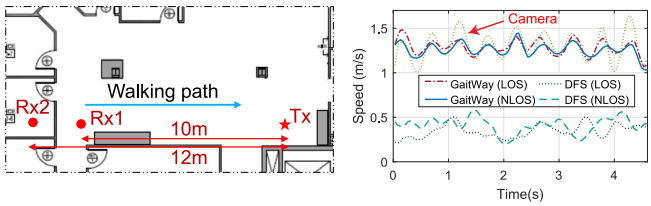

(a) Comparison setup (b) Speed estimation

Fig. 4. Comparison with DFS.

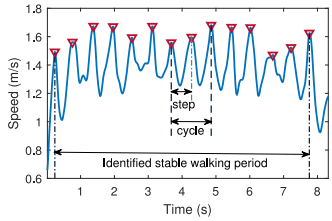

Fig. 6. Gait cycle estimation.

wall (12 m away), as shown in Fig. 4a. A user is asked to walk around, and the two receivers measure the CSI simultaneously. Fig. 4b depicts the speed estimated by GaitWay and DFS-based method, with the estimates by a camera as a comparison. As seen, GaitWay accurately captures the speed using either the LOS or NLOS link, preserving not only the average speed but also the precise in-step speed changes. The speed estimates on both links are highly consistent with each other. The DFS-based method, however, fails to capture the actual speeds in both LOS and NLOS scenarios.

As well-recognized in the literature, DFS-based approaches only estimate partial speed components along a particular direction towards the link and can do so only under good LOS conditions [39], [49]. Its performance degrades significantly under many realistic settings when the Tx and Rx are distant away, like in Fig. 4a. This also explains why the performance of the DFS-based method in our comparison is far from satisfactory and much worse than those reported in previous works [39], [49], which are obtained only under highly restricted scenarios.

4 Gait Extraction and Recognition

In this section, we present how to monitor and recognize gait from the estimated walking speeds. We first identify a segment of stable walking and extract distinct features from there for monitoring and recognition.

4.1 Identifying Stable Walking

Previous works usually only allow a user to walk at an approximately constant speed and assume all data are collected during stable walking [49], [58], [67]. Differently, GaitWay aims at acquiring gait information for free natural walking. A user, however, may perform various activities, including walking, sitting, standing, and typing, etc. A user will walk at different speeds, especially when one is starting to walk from standing still, making a turn, or about to stop, etc. During these periods, the walking speed does not necessarily reflect the most distinctive and stable gait characteristics. Hence, the first step for gait analysis and recognition is to identify a period of stable walking, during which a subject walks normally with a habitual pace.

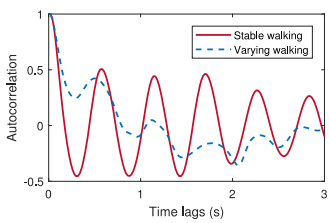

Fig. 5. ACF of walking speed.

We devise an algorithm that automatically detects a stable period during a user's normal activities. Our critical insight is that, when a user is walking smoothly, the observed speed will reach a certain range with repetitive patterns due to the periodic step rhythms.

We use the ACF of the speed to measure such walking periodicity. As shown in Fig. 5, when a user is walking stably, evident peaks will be observed from the ACF of the speed. In contrast, the ACF will be more flatted out for varying walking. We apply a sliding window (3 seconds) to the speed estimates and calculate the ACF for each window. We then employ peak detection on the ACF of the speed and examine the first peak. A period will be considered as stable walking only if a continuous series of reliable peaks are observed.

To be more robust, we further check the averaged center trend of the walking speed, which is obtained by smoothing the speed estimates with a relatively large window of 2 seconds. A walking period will be used for gait analysis only when the average speed is larger than a certain value (e.g., 0.7 m/s, which is smaller than normal human walking speed ranging from 1.0 m/s to 2.0 m/s). Fig. 7 illustrates an example of the identified stable walking periods. Each stable period then becomes a gait instance with a speed series $V = [v(t_i), i = 1, 2, \ldots, M]$.

4.2 Estimating Gait Cycles

A gait cycle is defined as the duration between two consecutive events that the same heel hits the ground during walking. In GaitWay, we estimate not only the gait cycle time but also segment the speed series for every individual step.

During normal human walking, a subject's speed will experience an increase followed by a decrease, resulting in a speed peak for each step. Therefore, we perform a simple peak detection on the speed series to identify steps, as shown in Fig. 6. To combat noises and outliers, we have applied certain constraints (including peak prominence and height) for peak detection. When all steps are identified, we trim the walking period by removing the duration before the first peak and after the last peak. The remained trace becomes a valid gait instance for further analysis in GaitWay.

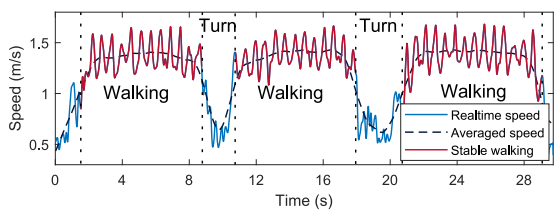

Fig. 7. Extracting stable walking period. The speed is measured when a user is walking along a 10-meter corridor for 3 times.

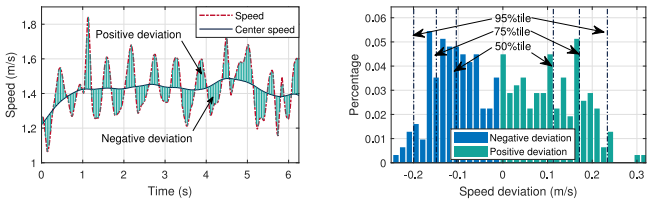

(a) Speed deviation (b) Deviation histogram

Fig. 8. Features of speed deviation.

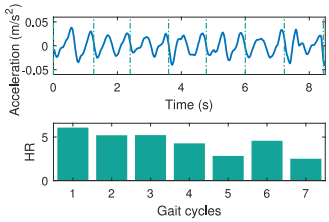

Fig. 10. Progression of harmonic ratios of a short walking trace.

4.3 Extracting Gait Features

Most of the previous works extract data-driven features directly from CSI measurements, which are implausible and contain environment-dependent features. As a consequence, all previous WiFi-based methods only work in restricted settings [27], [29], [49], [58], [63], [67]. Differently, GaitWay performs human identification by extracting true gait features, which are *physically plausible* and *environmentally irrelevant*, from the speed estimates. Following this notion, we devise a number of interpretable features to comprehensively characterize one's gait pattern from various aspects such as symmetry, smoothness, variability, and stability, etc., in addition to the straightforward physiological properties like speed, stride length, and gait cycle time.

Speed Deviation. The average walking speed is first taken as the mean value of instantaneous estimates of a user's walking speed. As shown in Fig. 9, our measurements demonstrate that not only do different users have different habitual speeds but also a user's walking speed varies over time. As a result, we only employ the average walking speed as a metric for gait speed assessment for a specific individual but do not use it as a classification feature. Instead, we exploit features that are more independent from the mean walking speed for recognition. As shown in Fig. 8a, we first detrend the absolute speed by subtracting the average center speed. Then we calculate the different percentile values (we take 95%tile, 75%tile, and 50%tile in GaitWay) of the speed deviations. Specifically, we take these percentile values of the positive deviations, negative deviations, and the absolutes of all deviations, respectively.

Gait Cycle Time. The gait cycle time is computed as the mean duration of every two consecutive steps. The middle row of Fig. 9 shows the average cycle time of two users' walking instances measured at different locations and time. Over 20 traces, variances of 0.7 ms and 0.6 ms are observed for the two users, respectively.

Stride Length. Stride estimation has been a long-standing challenging problem [57]. Thanks to the accurate speed estimation, we can intuitively derive the stride length by integrating the speed estimates over the time duration of each step. The bottom row of Fig. 9 depicts the estimated stride lengths for two users.

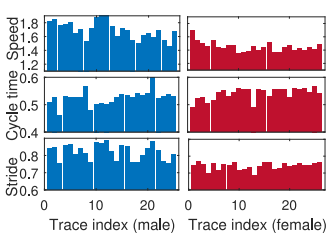

Fig. 9. Continuous monitoring of walking parameters over time.

Acceleration. Acceleration is computed as the derivatives of speed. We take the maximum, minimum, and variance of the acceleration. Since the walking acceleration also exhibits sinusoid-like patterns, we also identify the peaks and valleys of the acceleration sequence and compute the respective variances.

Smoothness. The harmonic ratio (HR) has been widely adopted as a quantitative measure of walking smoothness [2], [3]. HR examines the step-to-step symmetry within a stride by quantifying the harmonic composition of the accelerations for a given stride. It first conducts Discrete Fourier Transform (DFT) on the acceleration within each stride. The HR is then defined as the ratio of the sum of the amplitudes of the even harmonics to that of the odd harmonics. We use the first twenty harmonics to calculate the HRs, as justified for normal cadences for which the majority of the power occurs below 10 Hz [22]. Fig. 10 illustrates the HRs of a walking trace of 7 cycles (14 steps), demonstrating the progression of step-to-step symmetry during the walk. For every gait cycle during walking, we have one HR value. To obtain a single value feature for a walking trace, we take the median and variance of the HR values.

Rhythmicity. Recall Fig. 5, we calculate the ACF of the walking speed V. If a user walks in a regularly rhythmic manner, the speed ACF will exhibit multiple prominent peaks and will decay slowly. Hence the ACF embodies the walking rhythmicity or dynamic stability. We thus develop several features based on the ACF of the speed. In GaitWay, we apply a sliding window to calculate a series of ACF for each walking instance, resulting in a speed ACF matrix. From there, we perform peak detection on each column to find the prominent peak and the corresponding delay. We then extract the following single-valued features: The mean and variance of the heights of the first peaks and the number of identified prominent peaks; the variance of differences of peak locations for each column; and the ratio of columns in the matrix that does not have a prominent peak.

Symmetry. We calculate the step time and stride lengths of left and right foot[1] respectively, and take their means and standard deviations as features. The difference of each feature between two feet is derived as a measure of gait symmetry, which will not be affected whether odd steps are treated as the left foot or right foot.

1. Odd and oven steps are used here because of the lack of knowledge on the left and right foot. Although it might be easy to mistake the left foot with the right foot, the exchange of left/right stride lengths does not affect too much since most people walk relatively symmetrically.

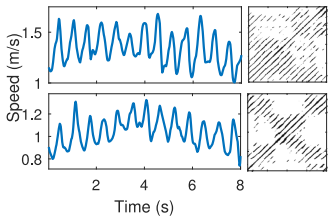

Fig. 11. Examples of RPs.

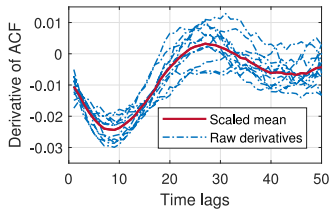

Fig. 12. Scaled ACF features.

RQA. To quantify the gait variability, we adopt Recurrence Quantification Analysis (RQA) [24], a method of nonlinear data analysis that quantifies the number and duration of recurrences of a dynamical system presented by its phase space trajectory using recurrent plot (RP). An RP is mathematically expressed as an N*N matrix R

$$R_{ij} = \Theta(\epsilon - ||\vec{x}_i - \vec{x}_j||), \vec{x}_i \in \mathbb{R}^m, i, j = 1, 2, \ldots, N,$$

where N is the number of states, ϵ is a predefined cutoff distance, $||\cdot||$ is a norm and $\Theta(\cdot)$ the Heaviside function. In GAITWAY, the state space trajectory X is constructed from the speed series $\{v_i, i = 1, 2, \ldots, L\}$ with an embedding dimension of 5 and a delay of 10 samples. Fig. 11 depicts two illustrative RPs for two different users, where the upper RP presents more diagonal lines, indicating a more stable and periodic gait.

A number of measures can be derived by RQA. We exploit the below four of them: (1) Recurrence rate: The percentage of recurrence points in an RP; (2) Determinism: The percentage of recurrence points that form diagonal lines; (3) The Shannon entropy of the probability distribution of the diagonal line lengths; and (4) The average diagonal line length.

Our measurements show that RQA reaches a stable value when calculated over 4 gait cycles, suggesting the shortest length for stable walking period detection. In practice, we relax the minimum to 3 cycles (i.e., 6 steps). Walking periods with less than 3 cycles are not considered for gait recognition but only for monitoring.

ACF Features. Finally, we also investigate the ACF of CSI (Fig. 2) for feature extraction. Since the ACF is entwined with walking speed yet is independent of location and environment, it can serve as a signature for gait classification. Specifically, rather than using all ACFs within a walking period, we consider the ACF corresponding to the speed peaks, as identified in Fig. 6. Note that the peak speeds could be different within a walking trace, i.e., the locations of the first peak of the ACF vary over time. Hence we aligned all the ACFs to a scale corresponding to the mean peak speed. To make it more apparent, we take the difference between each ACF and then average the aligned ACF differences. Fig. 12 illustrates an example of the scaled ACF differences. We use the first 50 taps as a feature vector in our system.

In GAITWAY, we focus on two subgoals: gait speed monitoring and recognition. To monitor and assess an individual's gait, we investigate three straight-forward and commonly used properties, i.e., average walking speed, gait cycle time, and stride length. We also use the harmonic ratio [2], a well-recognized measure for stability and symmetry, to evaluate gait progression.

To recognize a user, we fuse all the above features, resulting in a 90-dimensional feature vector for each gait instance. We conduct the following two steps for potential dimension deduction. First, we investigate whether these features are correlated with each other or not. We calculate the pair-wise correlations of all the features (except for the 50-dimensional ACF features that are taken as a whole). Then we eliminate one of each pair of highly correlated features for classification. Second, we employ an outcome-based approach for feature selection. Specifically, we perform 10-fold cross-validation with and without a specific feature and keep that feature only if it improves the output classification rate.

4.4 Recognizing Gait

Given the features that we have extracted, we now present how to identify a user (from others) by the gait patterns. Following the literature on gait recognition [8], we consider two identification scenarios: *single-user verification* that validates whether a user is the target subject or an unknown stranger, and *multiple user recognition* that identifies which target subject the user is among a set of candidates. We leverage Support Vector Machine (SVM), a widely-used classification technique, for this purpose. In GAITWAY, we use SVM instead of the popular deep learning techniques mainly because our primary goal is to demonstrate the effectiveness of the speed estimates and the plausible physical features for gait recognition. We keep applying deep learning to future work.

Single User Verification. For single-user verification, we train a gait model for the subject by building a binary classifier, which sees the subject's gait instances as a positive class and several benchmark users' as a negative class. The benchmark data could be obtained from available standard public database. In GAITWAY, they are randomly selected from our experiment participants. To authenticate the target person, we calculate the probability that an instance fits the target class. A testing gait instance is considered belonging to the target subject when the probability is higher than a threshold and is otherwise rejected. In practice, the threshold can be defined as different sensitive level by the users to adapt to different authentication applications.

Multiple User Recognition. To recognize multiple users, we train a one-vs-all binary classifier for each user, with the gait instances from this user as the positive class and the instances from all other candidates as the negative class. Then given a gait instance for testing, we feed it into every classifier and obtain the fitness probability that the instance belongs to each class. The gait instance is assigned to the user from whose classifier the highest fitness probability is observed.

We use LibSVM tool [6] with the Radial Basis Function (RBF) kernel. The optimal values for parameters γ and c are selected by grid search with 10-fold cross-validation. Features are scaled to [0,1] for classification.

We note that in this section and throughout the paper, the data are automatically collected and extracted when the

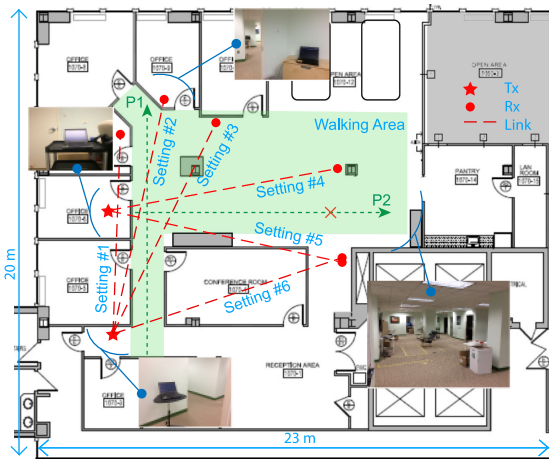

Fig. 13. Experimental areas and settings. Six settings of different Tx/Rx positions are tested. Under each setting, there is only one pair of Tx and Rx.

subject is walking around freely and naturally,[2] without being asked to walk along a predefined path or a predefined direction, nor to walk with deliberate speed. The Tx and Rx could be placed at arbitrary locations as long as they provide excellent coverage. More importantly, there is no need to retrain the system even if the positions of Tx and/or Rx change since the speed estimation is location independent, and all the features are extracted from the speed estimates. These are critical properties that underpin a ubiquitous gait monitoring and recognition system. It significantly differs from previous works that exert many of these constraints to testers in order to obtain environmentally repeatable features for human recognition [58], [62], [63] or to derive DFS [49].

5 Evaluation

5.1 Methodology

Experimental Settings. We implement GaitWay on commodity WiFi devices and conduct experiments in a typical building with an area of about 5, 000 ft^2. The floorplan of the experimental area is shown in Fig. 13. We consider different settings by placing the WiFi Tx and Rx at different locations (as roughly marked in Fig. 13) during multiple sessions of data collection. For each data session, there is only one single pair of Tx and Rx. Specifically, we have 6 different settings, where the Tx and Rx are put on a stand with a height of about 1 m. The Tx and Rx are separated by 8 to 11 meters for all settings, blocked by one or multiple walls. The Tx and Rx are both commercial laptops equipped with off-the-shelf WiFi network interface card (Intel 5300) and unmodified omni-directional chip antennas. We use the Linux 802.11n CSI Tool [16] to collect CSI measurements. We use 5.8 GHz channels (by default channel 161) with a bandwidth of 40 MHz. There are a number of WiFi devices co-existing on the same channel.

Data Collection. We collected gait instances from 11 human subjects, of which 5 are female, and 6 are male. During data collection, the users were walking around continuously and freely in their natural way. The user was free to walk through any area. Some of them read news, play mobile games, or talk on the phone while walking. During data collection, other people are working around but not walking. The experiments were conducted on 4 different days across six months. For each day, we collected data for two sessions at different times. We obtained 8 sessions of data in total, each under a different setting, as in Fig. 13. Users wore different clothes (from summer to autumn) during different sessions of data collection. For each session, we measured for about 10∼20 minutes of walking for each subject. The data were anonymized for privacy concerns.

In total, we collect about 1,030 minutes of walking data from the 11 participants, from which we extract around 970 minutes of walking (i.e., there are about 60 minutes during which a subject is out of effective coverage of the link, and the speed is not captured). From these data, we extract 5,283 gait instances of effective, stable walking, which occupies about 680 minutes, approximately 67% of the total walking duration. The effective percentage is limited in our data collection because users are walking freely as will with frequently stop-and-go and turning behaviors that could not serve as reliable gait measurements. In practice, the training data collection would be more efficient if the users are cooperative in gait measurements. Compare with many previous works that require the users to walk on a fixed pathway repeatedly, GaitWay greatly eases the task and boosts gait collection to a large scale.

Metrics. We separately study the performance of three cases: single-user verification, dual user distinction, a special case of multiple user recognition, and general multiple user recognition. Following the literature of gait recognition [8], we use the Receiver's Operating Curve (ROC) for the False Acceptance Rate (FAR) and False Rejection Rate (FRR), and the Equal Error Rate (EER), the point on the ROC where the FAR equals the FRR, to evaluate verification, and Recognition Rate (RR) for recognition evaluation. All the results below are obtained on a 10-fold validation basis.

5.2 Speed Estimation Performance

We first evaluate the performance of GaitWay in monitoring gait speed, for which the accuracy of speed estimation is the key. Considering both LOS and NLOS conditions, we set up two links, one Tx with two Rx. One Rx is 10 m away from the Tx, while the other is 12 m away behind a wall. Speed is estimated by each link individually. The user walks around naturally in the field of view of the camera. We evaluate with two users (one male and one female) for these experiments. We set up a camera to estimate the true speeds. We also implement the DFS-based speed estimation in [49].

As shown in Fig. 14a, GaitWay achieves remarkable accuracy, with a median error of 0.12 m/s and a 90%tile error of 0.35 m/s. The accuracy is ensured in both LOS and NLOS scenarios, with a marginal difference of 0.04 m/s in median error. The better performance in NLOS scenarios is attributed to the proposed statistical model, which holds better under NLOS with more uniformly distributed multipaths than LOS. We believe such accuracy provides clinically meaningful gait speed that was previously difficult to measure. As a comparison, the DFS-based approach fails to capture speeds due to limitations discussed in Section 3.1. As seen in Fig. 14a, DFS-based method produces a 0.9 m/s median and 1.24 m/s

2. We assume a user is walking naturally for recognition, which is a general assumption for gait recognition systems based on walking speed. If a user is walking strangely on purpose, carrying a heavy box, or moving a cart, GaitWay can still estimate the walking speeds, but it does not make sense to perform recognition upon the distorted speeds.

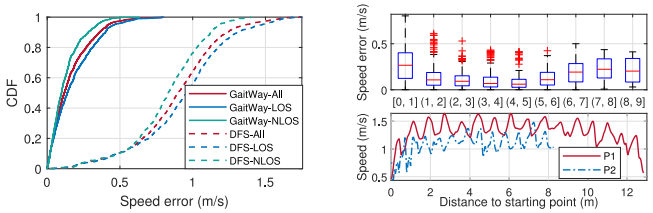

(a) Accuracy (b) Coverage

Fig. 14. Performance of speed estimation.

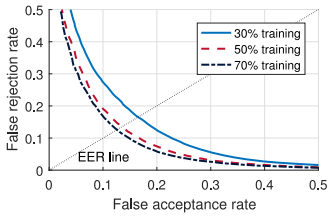

Fig. 15. ROC with % of training samples.

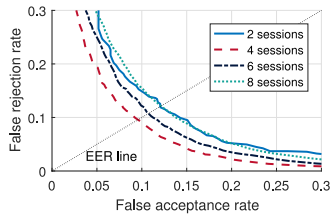

Fig. 16. ROC with data sessions.

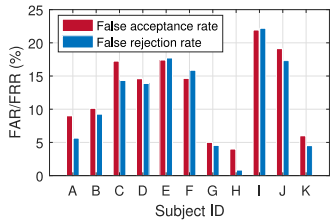

Fig. 17. Verification for different users.

90%tile error, about 64 and 89% in relative errors considering the true average speed is about 1.4 m/s.

We also study the coverage that GaitWay can reliably track a user's moving speed. To do so, we first analyze the speed estimation accuracy with respect to the distance traveled using the above data. As illustrated in Fig. 14b, the median errors are consistently below 0.2m/s for all ranges except for the beginning period. Large errors during the first meter arise from the unstable walking behavior that causes distortions in camera-based speed tracking. We perform further experiments to study the coverage that GaitWay can detect the speed. Rather than asking a user to walk freely, we now let the user walk along two specific paths (P1 and P2), both about 12 m long, and collect data under Setting #2, as shown in Fig. 13. We test with multiple users, each repeating for 10 times, and the results show a consistent coverage. We illustrate two examples and plot the speed estimates with respect to the distance a user has traveled from the starting location in Fig. 14b. As seen, GaitWay estimates the walking speed very well throughout the entire path of P1, which is under good coverage of the link in Setting #2. As a comparison, GaitWay tracks the speed until the point the user has walked for about 8.5 m (as marked by the red cross in Fig. 13), where the user is already about 9 m from the Rx and 11 m from the Tx, respectively. For further locations, the scattering signals through multiple walls are too weak for GaitWay to perform reliable estimation. The coverage is as expected accordingly to the theoretical coverage shape of the Cassini ovals for passive human sensing [38]. Yet as long as GaitWay can detect the walking, it outputs accurate speed estimates and thereby underpins recognition.

Based on the delightful instantaneous speeds, GaitWay can monitor various parameters like steps and stride lengths. In particular, over 10 segments of walking, GaitWay correctly counts the steps with less than 1 step errors for 9 of them and a 2-step error for the other one. Most of the errors occur at the beginning or end of a walk. For the identified steps, GaitWay estimates stride lengths accuracy (thanks to the accurate speed estimates), with a respective 2.36 cm and 4.03 cm mean errors for the female and male user compared to camera-based results. We cannot obtain steps and strides from the DFS-based method due to the low-quality speed estimates. For the same reason, we do not further compare with it for gait recognition [49].

5.3 Recognition Performance

Single User Verification. To evaluate the performance of GaitWay for verification, we test each subject in our dataset by using the gait instances of all other users as a negative class. We shuffle the training and testing data for 10 folds and depict the integrated results. As shown in Fig. 15, GaitWay achieves an EER of 12.58% when using 70% of gait instances for training. The EER will increase by about 1 and 3% when shrinking the training size to 50 and 30%, respectively. We study the performance with respect to temporal changes in Fig. 16. As seen, the performance slightly degrades when more sessions over time are involved. The best EER of 9.57% is achieved when using the first 4 sessions. The performance using 2 sessions is worse than using more sessions because there is not sufficient data for training when using the first 2 sessions. Fig. 17 shows the FAR and FRR for each user with all sessions of data.

Two User Distinction. Before evaluating multiple user recognition, it is interesting to study a special scenario of two users since it is common in practice that two persons share an office room or two residents live in one apartment. It would be particularly useful if we can distinguish one from another. Thus we conduct binary classification for every pair of subjects in our dataset. To better understand the results, we consider precision and recall by treating one user as the positive class and the other as the negative class for each group. As shown in Fig. 18, GaitWay yields remarkable performance, with an average precision and recall of 94.84 and 95.21% respectively for 55 pairs of users when using 70% of data for training. And the accuracy of $>90\%$ can be achieved with only 20% of data for training. With our automatic data collection and gait extraction, such an amount of data can be easily gathered by a walk of about 20 minutes, making GaitWay friendly for user enrollment.

Multiple User Recognition. The recognition for multiple users is much more complicated than verification or pair distinction. As shown in Fig. 19, the RR, when using 70% of data over all sessions for training and the others for testing, is

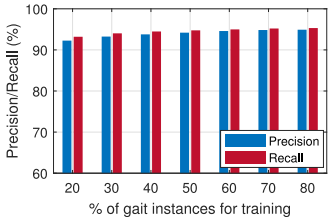

Fig. 18. Two user distinction.

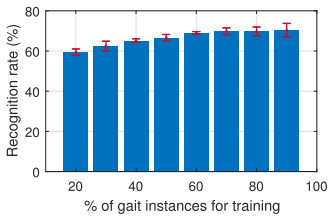

Fig. 19. RR versus size of training samples.

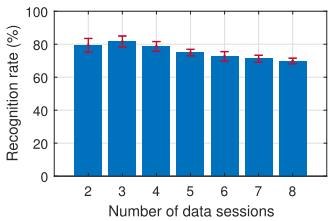

Fig. 20. RR versus # of data sessions.

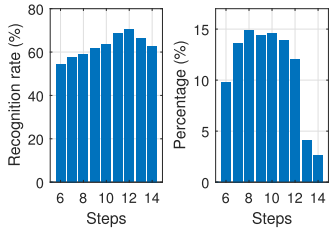

Fig. 21. RR versus length of gait instances.

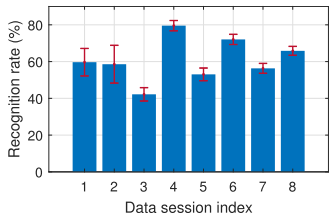

Fig. 22. RR versus data session.

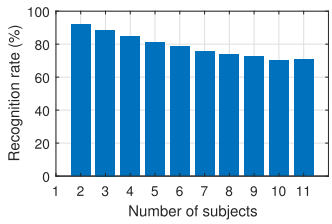

Fig. 23. RR versus number of users.

69.84% for 11 users, which decreases to 66.63% with half of the data for training. The performance is comparable to the start-of-the-art works based on wearable sensors [64], [66], which report a respective RR of 66.3 and 73.4% on two sessions of data with accelerometers.

Gait Variations. Fig. 20 illustrates how the RR changes with gait variations when involving different sessions. As seen, the performance degrades from 81.59% when using the 3 sessions from the first two days to 69.84% when using all 8 sessions of data. This is because a user's gait speed may vary considerably over time. For example, one user in our experiments had a walking speed of about 0.8 m/s in one session while about 1.4 m/s in another session. Although GaitWay circumvents the use of absolute speed, the performance may still be influenced by dramatic changes in walking speed since our system is built upon walking speed alone. Unless otherwise specified, we use all 8 sessions of data in the following evaluation.

Gait Instance Length. As our data are collected and extracted automatically, the duration and step amounts of each gait instance would be different. We thus analyze whether the lengths of walking samples will affect recognition accuracy. We analyze the length distribution of all testing gait instances, as shown in the right part of Fig. 21, and depict the corresponding RRs in the left part. As seen, we are able to identify a user who just walks six steps. The RR tops the best of 70.52% for gait instances of 12 steps and decreases for either longer or shorter instances. A subject's gait may vary for a long walking, which should thus be partitioned into appropriate instances. For example, the trace can be automatically segmented into instances of around 12 steps, which will produce better accuracy. Thus GaitWay will do the instance segmentation automatically, and there is no need for a user to pay attention to the trace length.

Data Sessions. We study the impact of different sessions/settings in Fig. 22. While most of the data sessions produce similar performance, session #3 sees the worst performance of only 42.19%. This is because the Rx is too close to a reinforced concrete pillar of about 1 m $\times$ 1 m, and thus the weak scattering signals from the human body can hardly be received. Under such conditions, even with MRC, it cannot recover the speed signals well. However, WiFi devices are usually placed to achieve good coverage, and such a rigorous situation would be avoided. GaitWay only needs one single pair of WiFi radios. In practice, however, if multiple pairs are used to monitor a large area, it is suggested to deploy relatively densely and then, for locations covered by multiple pairs, the information could be aggregated to improve accuracy.

Number of Subjects. To study the impacts of subject number registered in the database, we traverse all 2,036 possible groupings of the 11 subjects, with group sizes increasing from 2 to 11, and integrate the results in Fig. 23. In general, the RR gradually decreases with more users being involved. However, we note that GaitWay retains a remarkable RR of over 80% when there are 5 subjects, demonstrating the promising potential for the smart home where there are usually a few residents in a house.

Subject Diversity. Fig. 24 shows the confusion matrix of 11 subjects with data sessions across four days. Most of the subjects experience RRs higher than 65%, except for subject E and subject I, who are very similar to each other. Comparing Figs. 24 and 17, subjects with lower RRs also suffer from relatively larger FAR and FRR among others, indicating that their gait patterns are less distinctive.

Comparative Study. Our performance is similar to previous works based on wearable sensors [8], [64], [66], which report

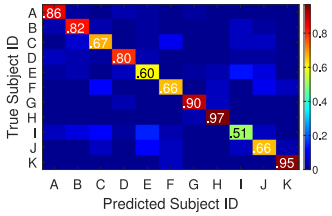

Fig. 24. Recognition confusion matrix.

EERs from 5 to 20%, mostly based on only one or two sessions of data. GAITWAY outperforms or is comparable to the state-of-the-art CSI-based methods, including WiWho [58] that reports 92 to 80% RR for 2 to 6 users respectively and WifiU [49] that achieves an EER of 8.6%. Applying sophisticated machine learning techniques, CrossSense [62] considers three sites and reports an accuracy of over 80%, while reports $<20\%$ for WiWho and WifiU. The data, however, is collected in a single session on each site. Again, all of them are confined to a fixed straight path in a predefined direction within a narrow LOS area. In contrast, GAITWAY is evaluated in through-the-wall scenes with distant Tx and Rx in which none of these systems can work.

Although GAITWAY tops the performance regarding accuracy and practicability among WiFi-based approaches, the recognition accuracy is not super high. An important reason is that GAITWAY uses gait speed alone, which is less distinct and reliable than many other biometric traits such as body shape and foot size and shape, etc. Thus we mainly envision GAITWAY as a ubiquitous solution for daily applications but not for critical human identification.

5.4 Latency

We evaluate the Matlab code of GAITWAY on a laptop equipped with an Intel Core i7. GAITWAY can run in realtime on personal computers. For 1 minute of data, it takes about 27 seconds (20s for speed estimation, 6s for stable period identification, and $<$ 1s for feature extraction) to process. SVM takes 164s and 2s for training and testing with 1,000 instances, respectively. As training can be done offline, this cost is negligible. In addition, note that there is also data collection latency from the entire system perspective since a user needs to keep walking for a minimum of 6 steps (recall Fig. 21) for recognition.

5.5 Limitations and Future Work

While GAITWAY significantly advances the state-of-the-art in WiFi-based gait recognition, it has several limitations. First, GAITWAY can only estimate the speed of a single walking user with or without other users around but not walking). In the case of multiple people walking, it will produce a synthesized speed but cannot separate them due to the fundamental limits of antenna number and frequency bandwidth on 2.4 GHz/5 GHz WiFi. Thus the present solution is not suitable for recognizing multiple concurrent walking users. Second, the current implementation uses a high sampling rate of 1500 Hz. Third, while we have demonstrated the remarkable performance of GAITWAY, our recognition experiments are currently limited to 11 users due to budget constraints. Our future work extends to a larger group of users and explores lower sampling rates as well as multi-person scenarios. Future work also includes building neural network models for gait recognition by using the distinct speed estimates.

6 Related Works

To monitor gait as a vital indicator, clinicians mainly measure gait speed. Yet gait recognition would demand more extensive information related to an individual's walking style and her biometric traits (e.g., body mass and shape, foot size and shape, etc.). Traditionally, gait speed is measured manually by a physician by asking the subject to walk for a certain distance and measuring the corresponding walking time. Commercial systems like VICON (based on a set of infrared cameras) or GAITRite (based on pressure mats) are nowadays used in some medical settings. The literature on automating the acquisition of gait information more inexpensively has dramatically grown recently.

Vision. Vision-based approaches rely on multi-view images of gait captured by an array of cameras to produce high recognition rates [65]. A standard and effective method of representing vision-based gait is the average silhouettes formed by a sequence of images [17]. Depth cameras such as Kinect has also been explored for in-home gait monitoring recently [44]. In addition to the complex and cumbersome infrastructure, vision-based approaches are vulnerable to various factors, including viewing angles, surrounding conditions, and the subject's apparel and accessories. They are also undesirable for in-home use due to privacy concerns.

Pressure. Underfoot pressure is also widely investigated, which is measured by floor sensors such as a force plate [32] or a pressure mat [7], [34]. Pressure mats capture spatial and temporal gait features dictated by foot size and geometric shape, orientation, and inter-footstep properties (e.g., toe-out angle), etc. Pressure sensors, however, require direct contact with foot and may degrade for shod walking since various footwear would redistribute the force of the foot differently. Acoustic sensors [15] and vibration sensors [37] are also used to capture footstep-induced sound and floor vibration for recognition, respectively. Similar to underfoot pressure, they are also susceptible to footwear, walking speed, and ambient noises. Moreover, all of the above systems, using cameras or floor sensors, require complicated installation of dedicated devices, limiting their use in restricted areas. Yet in spite of this, these works have objectively affirmed the feasibility of gait recognition even for a large set of subjects.

Acceleration. To achieve continuous gait monitoring and recognition, inertial sensors, especially those built in smartphones and wearables, are explored to record accelerations during gait [64], [66]. Reasonable recognition rates could be achieved when placing multiple sensors on different body locations [64]. Inertial sensing, however, is well-know to be noisy and vulnerable and is incapable of measuring walking speed. Wearable sensors are also unfavorable, especially to elderly people.

Radio. Different from the above works, GAITWAY monitors a subject's gait speed and further recognizes her from the ambient radio signals reflected off her body, passively and unobtrusively. Existing works measure walking speed either by using specialized low-power radar signals [20], [46], or by extracting Doppler frequency shifts from WiFi signals [25], [39], [40], [49]. These works, however, require the user to walk on a predefined path in a predefined direction, with WiFi transceivers placed at fixed locations, and only work in restricted scenarios with clear LOS conditions. Moreover, as Doppler shifts only relate to partial speed component

projected in a specific direction, the measured speed may be incorrect if the user deviates from the designated path. Other works directly extract certain signal features and match against prior trained database to classify human [26], [27], [29], [55], [56], [58], [62], [63], [67] or activities [10], [11], [13], [21], [28], [48], [51], [52], [54], [59]. Neither can they measure gait speed, nor do they sense physically interpretable characteristics related to gait. In addition, none of these systems work through the walls as GAITWAY does.

7 CONCLUSION

GAITWAY is the first system that can monitor and recognize gait through the walls using commodity WiFi signals. It continuously measures speed passively and unobtrusively and extracts physically plausible features of the speed for gait recognition. We validate the real-world performance and demonstrate that it operates well when a user is 10 m away from the link behind the walls. The proposed scattering model underpinning such through-the-wall capability offers new exciting directions and opportunities for wireless sensing.

REFERENCES

[1] A. Alfaro-Acha, S. Al Snih, M. A. Raji, K. S. Markides, and K. J. Ottenbacher, "Does 8-foot walk time predict cognitive decline in older mexicans americans?" *J. Amer. Geriatrics Soc.*, vol. 55, no. 2, pp. 245–251, 2007.

[2] J. L. Bellanca, K. A. Lowry, J. M. Vanswearingen, J. S. Brach, and M. S. Redfern, "Harmonic ratios: A quantification of step to step symmetry," *J. Biomechanics*, vol. 46, no. 4, pp. 828–831, Feb. 2013.

[3] M. C. Bisi, F. Riva, and R. Stagni, "Measures of gait stability: Performance on adults and toddlers at the beginning of independent walking," *J. NeuroEng. Rehabil.*, vol. 11, Sep. 2014, Art. no. 131.

[4] M.-V. Castell, M. Sánchez, R. Julián, R. Queipo, S. Martín, and Á. Otero, "Frailty prevalence and slow walking speed in persons age 65 and older: Implications for primary care," *BMC Family Pract.*, vol. 14, no. 1, Art. no. 86, 2013.

[5] M. Cesari *et al.*, "Prognostic value of usual gait speed in well-functioning older people-results from the health, aging and body composition study," *J. Amer. Geriatrics Soc.*, vol. 53, no. 10, pp. 1675–1680, 2005.

[6] C.-C. Chang and C.-J. Lin, "LIBSVM: A library for support vector machines," *ACM Trans. Intell. Syst. Technol.*, vol. 2, pp. 27:1–27:27, 2011. [Online]. Available: http://www.csie.ntu.edu.tw/cjlin/libsvm

[7] Y.-O. Cho, B.-C. So, and J.-W. Jung, "User recognition using sequential footprints under shoes based on mat-type floor pressure sensor," *Adv. Sci. Lett.*, vol. 9, no. 1, pp. 591–596, 2012.

[8] P. Connor and A. Ross, "Biometric recognition by gait: A survey of modalities and features," *Comput. Vis. Image Understanding*, vol. 167, pp. 1–27, Feb. 2018.

[9] J. E. Cutting and L. T. Kozlowski, "Recognizing friends by their walk: Gait perception without familiarity cues," *Bull. Psychonomic Soc.*, vol. 9, no. 5, pp. 353–356, 1977.

[10] S. Depatla and Y. Mostofi, "Crowd counting through walls using WiFi," in *Proc. IEEE Int. Conf. Pervasive Comput. Commun.*, 2018, pp. 1–10.

[11] S. Depatla and Y. Mostofi, "Passive crowd speed estimation and head counting using WiFi," in *Proc. 15th Annu. IEEE Int. Conf. Sens. Commun. Netw.*, 2018, pp. 1–9.

[12] H. El-Alfy, I. Mitsugami, and Y. Yagi, "A new gait-based identification method using local gauss maps," in *Proc. Asian Conf. Comput. Vis.*, 2014, pp. 3–18.

[13] B. Fang, N. D. Lane, M. Zhang, A. Boran, and F. Kawsar, "BodyScan: Enabling radio-based sensing on wearable devices for contactless activity and vital sign monitoring," in *Proc. 14th Annu. Int. Conf. Mobile Syst. Appl. Services*, 2016, pp. 97–110.

[14] S. Fritz and M. Lusardi, "White paper: Walking speed: The sixth vital sign," *J. Geriatric Physical Therapy*, vol. 32, no. 2, 2009, Art. no. 2.

[15] J. T. Geiger, M. Hofmann, B. Schuller, and G. Rigoll, "Gait-based person identification by spectral, cepstral and energy-related audio features," in *Proc. IEEE Int. Conf. Acoust. Speech Signal Process.*, 2013, pp. 458–462.

[16] D. Halperin, W. Hu, A. Sheth, and D. Wetherall, "Tool release: Gathering 802.11 n traces with channel state information," *ACM SIGCOMM Comput. Commun. Rev.*, vol. 41, no. 1, pp. 53–53, 2011.

[17] J. Han and B. Bhanu, "Statistical feature fusion for gait-based human recognition," in *Proc. IEEE Comput. Soc. Conf. Comput. Vis. Pattern Recognit.*, 2004, pp. II–II.

[18] J. Han and B. Bhanu, "Individual recognition using gait energy image," *IEEE Trans. Pattern Anal. Mach. Intell.*, vol. 28, no. 2, pp. 316–322, Feb. 2006.

[19] D. A. Hill, *Electromagnetic Fields in Cavities: Deterministic and Statistical Theories*, vol. 35. Hoboken, NJ, USA: Wiley, 2009.

[20] C.-Y. Hsu, Y. Liu, Z. Kabelac, R. Hristov, D. Katabi, and C. Liu, "Extracting gait velocity and stride length from surrounding radio signals," in *Proc. CHI Conf. Hum. Factors Comput. Syst.*, 2017, pp. 2116–2126.

[21] W. Jiang *et al.*, "Towards environment independent device free human activity recognition," in *Proc. 24th Annu. Int. Conf. Mobile Comput. Netw.*, 2018, pp. 289–304.

[22] J. Kavanagh, S. Morrison, and R. Barrett, "Coordination of head and trunk accelerations during walking," *Eur. J. Appl. Physiol.*, vol. 94, no. 4, pp. 468–475, 2005.

[23] D. Levine, J. Richards, and M. W. Whittle, *Whittle's Gait Analysis (Fifth Edition)*. Amsterdam, Netherlands: Elsevier Health Sciences, 2012.

[24] X. Li, G. Ouyang, X. Yao, and X. Guan, "Dynamical characteristics of pre-epileptic seizures in rats with recurrence quantification analysis," *Phys. Lett. A*, vol. 333, no. 1/2, pp. 164–171, 2004.

[25] X. Li *et al.*, "IndoTrack: Device-free indoor human tracking with commodity Wi-Fi," in *Proc. ACM Interactive Mobile Wearable Ubiquitous Technol.*, 2017, vol. 1, Art. no. 72.

[26] Y. Li and T. Zhu, "Gait-based Wi-Fi signatures for privacy-preserving," in *Proc. 11th ACM Asia Conf. Comput. Commun. Secur.*, 2016, pp. 571–582.

[27] C. Lin, J. Hu, Y. Sun, F. Ma, L. Wang, and G. Wu, "WiAU: An accurate device-free authentication system with ResNet," in *Proc. 15th Annu. IEEE Int. Conf. Sens. Commun. Netw.*, 2018, pp. 1–9.

[28] K. J. R. Liu and B. Wang, *Wireless AI: Wireless Sensing, Positioning, IoT, and Communications*. Cambridge, U.K.: Cambridge Univ. Press, 2019.

[29] J. Lv, W. Yang, D. Man, X. Du, M. Yu, and M. Guizani, "Wii: Device-free passive identity identification via WiFi signals," in *Proc. IEEE Global Commun. Conf.*, 2017, pp. 1–6.

[30] A. Middleton, S. L. Fritz, and M. Lusardi, "Walking speed: The functional vital sign," *J. Aging Physical Activity*, vol. 23, no. 2, pp. 314–322, Apr. 2015.

[31] M. Montero-Odasso *et al.*, "Gait velocity as a single predictor of adverse events in healthy seniors aged 75 years and older," *The J. Gerontology Series A, Biol. Sci. Med. Sci.*, vol. 60, no. 10, pp. 1304–1309, 2005.

[32] S. P. Moustakidis, J. B. Theocharis, and G. Giakas, "Subject recognition based on ground reaction force measurements of gait signals," *IEEE Trans. Syst., Man, Cybern., B Cybern.*, vol. 38, no. 6, pp. 1476–1485, Dec. 2008.

[33] M. P. Murray, "Gait as a total pattern of movement: Including a bibliography on gait," *Amer. J. Phys. Med. Rehabil.*, vol. 46, no. 1, pp. 290–333, 1967.

[34] K. Nakajima, Y. Mizukami, K. Tanaka, and T. Tamura, "Footprint-based personal recognition," *IEEE Trans. Biomed. Eng.*, vol. 47, no. 11, pp. 1534–1537, Nov. 2000.

[35] The Administration for Community Living, "Profile of older Americans," 2017. [Online].Available: https://acl.gov/sites/default/files/Aging%20and%20Disability%20in%20America/2017OlderAmericansProfile.pdf

[36] The Japan Times, "Japan census report shows surge in elderly population, many living alone," 2016. [Online] Available: https://www.japantimes.co.jp/news/2016/06/29/national/japan-census-report-shows-surge-elderly-population-many-living-alone/

[37] S. Pan *et al.*, "FootprintID: Indoor pedestrian identification through ambient structural vibration sensing," in *Proc. ACM Interactive Mobile Wearable Ubiquitous Technol.*, 2017, vol. 1, Art. no. 89.

[38] N. Patwari and J. Wilson, "Spatial models for human motion-induced signal strength variance on static links," *IEEE Trans. Inform. Forensics Secur.*, vol. 6, no. 3, pp. 791–802, Sep. 2011.

[39] K. Qian, C. Wu, Z. Yang, Y. Liu, and K. Jamieson, "Widar: Decimeter-level passive tracking via velocity monitoring with commodity Wi-Fi," in *Proc. 18th ACM Int. Symp. Mobile Ad Hoc Netw. Comput.*, 2017, Art. no. 6.

[40] K. Qian, C. Wu, Y. Zhang, G. Zhang, Z. Yang, and Y. Liu, "Widar2. 0: Passive human tracking with a single Wi-Fi link," *Proc. 16th Annu. Int. Conf. Mobile Syst. Appl. Services*, 2018, pp. 350–361.
[41] O. C. Reyes, R. Vera-Rodriguez, P. Scully, and K. B. Ozanyan, "Analysis of spatio-temporal representations for robust footstep recognition with deep residual neural networks," *IEEE Trans. Pattern Anal. Mach. Intell.*, vol. 41, no. 2, pp. 285–296, Feb. 2019.
[42] R. H. Shumway and D. S. Stoffer, "Time series regression and exploratory data analysis," in *Time Series Analysis and its Applications*. Berlin, Germany: Springer, 2011, pp. 47–82.
[43] B. Sklar, *Digital Communications*, vol. 2. Upper Saddle River, NJ, USA: Prentice Hall, 2001.
[44] E. E. Stone and M. Skubic, "Unobtrusive, continuous, in-home gait measurement using the microsoft kinect," *IEEE Trans. Biomed. Eng.*, vol. 60, no. 10, pp. 2925–2932, Oct. 2013.
[45] S. Studenski *et al.*, "Gait speed and survival in older adults," *J. Amer. Med. Assoc.*, vol. 305, no. 1, pp. 50–58, 2011.
[46] D. Tahmoush and J. Silvious, "Radar micro-doppler for long range front-view gait recognition," in *Proc. IEEE Int. Conf. Biometrics: Theory Appl. Syst.*, 2009, pp. 1–6.
[47] D. Tse and P. Viswanath, *Fundamentals of Wireless Communication*. Cambridge, U.K.: Cambridge Univ. Press, 2005.
[48] B. Wang, Q. Xu, C. Chen, F. Zhang, and K. J. R. Liu, "The promise of radio analytics: A future paradigm of wireless positioning, tracking, and sensing," *IEEE Signal Process. Mag.*, vol. 35, no. 3, pp. 59–80, May 2018.
[49] W. Wang, A. X. Liu, and M. Shahzad, "Gait recognition using WiFi signals," in *Proc. ACM Int. Joint Conf. Pervasive Ubiquitous Comput.*, 2016, pp. 363–373.
[50] W. Wang, A. X. Liu, M. Shahzad, K. Ling, and S. Lu, "Understanding and modeling of WiFi signal based human activity recognition," in *Proc. Annu. Int. Conf. Mobile Comput. Netw.*, 2015, pp. 65–76.
[51] Y. Wang, J. Liu, Y. Chen, M. Gruteser, J. Yang, and H. Liu, "E-eyes: Device-free location-oriented activity identification using fine-grained WiFi signatures," in *Proc. 20th Annu. Int. Conf. Mobile Comput. Netw.*, 2014, pp. 617–628.
[52] N. Xiao, P. Yang, Y. Yan, H. Zhou, and X. Li, "Motion-fi: Recognizing and counting repetitive motions with passive wireless backscattering," in *Proc. IEEE Conf. Comput. Commun.*, 2018, pp. 2024–2032.
[53] Y. Xie, Z. Li, and M. Li, "Precise power delay profiling with commodity Wi-Fi," *IEEE Trans. Mobile Comput.*, vol. 18, no. 6, pp. 1342–1355, Jun. 2019.
[54] Y. Xie, Y. Zhang, J. C. Liando, and M. Li, "SWAN: Stitched Wi-Fi antennas," in *Proc. 24th Annu. Int. Conf. Mobile Comput. Netw.*, 2018, pp. 51–66.
[55] Q. Xu, Y. Chen, B. Wang, and K. J. R. Liu, "Radio biometrics: Human recognition through a wall," *IEEE Trans. Inf. Forensics Security*, vol. 12, no. 5, pp. 1141–1155, May 2017.
[56] Y. Xu, M. Chen, W. Yang, S. Chen, and L. Huang, "Attention-based walking gait and direction recognition in Wi-Fi networks," Nov. 2018, *arXiv: 1811.07162 [cs]*.
[57] Z. Yang, C. Wu, Z. Zhou, X. Zhang, X. Wang, and Y. Liu, "Mobility increases localizability: A survey on wireless indoor localization using inertial sensors," *ACM Comput. Surveys*, vol. 47, no. 3, 2015, Art. no. 54.
[58] Y. Zeng, P. H. Pathak, and P. Mohapatra, "WiWho: WiFi-based person identification in smart spaces," in *Proc. 15th ACM/IEEE Int. Conf. Inf. Process. Sensor Netw.*, 2016, pp. 1–12.
[59] D. Zhang, H. Wang, and D. Wu, "Toward centimeter-scale human activity sensing with Wi-Fi signals," *Computer*, vol. 50, no. 1, pp. 48–57, 2017.
[60] F. Zhang, C. Chen, B. Wang, and K. J. R. Liu, "WiSpeed: A statistical electromagnetic approach for device-free indoor speed estimation," *IEEE Internet Things J.*, vol. 5, no. 3, pp. 2163–2177, Jun. 2018.
[61] F. Zhang *et al.*, "SMARS: Sleep monitoring via ambient radio signals," *IEEE Trans. Mobile Comput.*, to be published, doi: 10.1109/TMC.2019.2939791.
[62] J. Zhang, Z. Tang, M. Li, D. Fang, P. Nurmi, and Z. Wang, "CrossSense: Towards cross-site and large-scale WiFi sensing," in *Proc. 24th Annu. Int. Conf. Mobile Comput. Netw.*, 2018, pp. 305–320.
[63] J. Zhang, B. Wei, W. Hu, and S. S. Kanhere, "WiFi-ID: Human identification using WiFi signal," in *Proc. IEEE Int. Conf. Distrib. Comput. Sensor Syst.*, 2016, pp. 75–82.
[64] Y. Zhang, G. Pan, K. Jia, M. Lu, Y. Wang, and Z. Wu, "Accelerometer-based gait recognition by sparse representation of signature points with clusters," *IEEE Trans. Cybern.*, vol. 45, no. 9, pp. 1864–1875, Sep. 2015.
[65] S. Zheng, J. Zhang, K. Huang, R. He, and T. Tan, "Robust view transformation model for gait recognition," in *Proc. 18th IEEE Int. Conf. Image Process.*, 2011, pp. 2073–2076.
[66] Y. Zhong and Y. Deng, "Sensor orientation invariant mobile gait biometrics," in *Proc. IEEE Int. Joint Conf. Biometrics*, 2014, pp. 1–8.
[67] H. Zou, Y. Zhou, J. Yang, W. Gu, L. Xie, and C. J. Spanos, "WiFi-based human identification via convex tensor shapelet learning," in *Proc. 32nd AAAI Conf. Artif. Intell.*, 2018, pp. 1711–1719.

Chenshu Wu (Member, IEEE) received the BE degree from the School of Software and the PhD degree from the Department of Computer Science, both from Tsinghua University, Beijing, China, in 2010 and 2015, respectively. He is currently an assistant research scientist with the Department of Electrical and Computer Engineering, University of Maryland, College Park, and a principal scientist at Origin Wireless Inc. His research interests include the Internet of Things and mobile computing. He is a member of the ACM.

Feng Zhang (Member, IEEE) received the BS and MS degrees from the Department of Electronic Engineering and Information Science, University of Science and Technology of China, Hefei, China, in 2011 and 2014, respectively, and the PhD degree from the Department of Electrical and Computer Engineering, University of Maryland, College Park, in 2018. He is currently with Origin Wireless, Inc. His research interests include wireless sensing, statistical signal processing, and wireless indoor localization. He was the recipient of Distinguished TA Award from the University of Maryland and the State Scholarship from the University of Science and Technology of China.

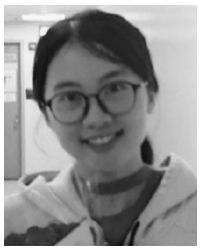

Yuqian Hu (Student Member, IEEE) received the BS degree from the Department of Electronic Engineering and Information Science, University of Science and Technology of China, Hefei, China, in 2017. She is currently working toward the PhD degree with the Department of Electrical and Computer Engineering, University of Maryland, College Park, Maryland. Her current research interests include statistical signal processing and wireless sensing. She was a recipient of the Graduate School Fellowship from the University of Maryland, College Park.

K. J. Ray Liu (Fellow, IEEE) is currently a Distinguished University professor and a Distinguished Scholar-Teach of University of Maryland, College Park, Maryland, where he is also Christine Kim Eminent professor of Information Technology. He leads the Maryland Signals and Information Group conducting research encompassing broad areas of information and communications technology with recent focus on wireless AI for indoor tracking and wireless sensing. He was a recipient of the 2016 IEEE Leon Kirchmayer Award on graduate teaching and mentoring, IEEE Signal Processing Society 2014 Society Award, IEEE Signal Processing Society 2009 Technical Achievement Award, and over a dozen of best paper awards. He is recognized by Web of Science as a Highly Cited Researcher. As the founder of Origin Wireless, his invention won the 2017 CEATEC Grand Prix award and CES 2020 Innovation Award. He is a fellow of AAAS, and National Academy of Inventors. He was IEEE vice president, Technical Activities, and a member of IEEE Board of Director as Division IX Director. He has served as president of IEEE Signal Processing Society, where he was vice president Publications and Board of Governor. He has also served as the editor-in-chief of the *IEEE Signal Processing Magazine*. He also received teaching and research recognitions from University of Maryland including university-level Invention of the Year Award; and college-level Poole and Kent Senior Faculty Teaching Award, Outstanding Faculty Research Award, and Outstanding Faculty Service Award, all from A. James Clark School of Engineering.